Domain unfolding in neurofilament sidearms: effects of phosphorylation and ATP

Helim Aranda-Espinoza[a,1,*], Philippe Carl[b,1], Jean-François Leterrier[c], Paul Janmey[a], Dennis E. Discher[a,b]

[a] *Institute for Medicine and Engineering, 1080 Vagelos Research Laboratory, 3340 Smith Walk, University of Pennsylvania, Philadelphia, PA 19104, USA*
[b] *Biophysical Engineering Laboratory, Department of Chemical and Biomolecular Engineering, University of Pennsylvania, Philadelphia, PA 19104, USA*
[c] *UMR 6558 CNRS, Poitiers, France*

Received 7 August 2002; revised 27 September 2002; accepted 29 September 2002

First published online 10 October 2002

Edited by Amy McGough

Abstract Lateral projections of neurofilaments (NF) called sidearms (SA) affect axon stability and caliber. SA phosphorylation is thought to modulate inter-NF distance and interactions between NF and other subcellular organelles. SA were probed by atomic force microscopy (AFM) and dynamic light scattering (DLS) as a function of phosphorylation and ATP content. DLS shows SA are larger when phosphorylated, and AFM shows four unfoldable domains in SA regardless of phosphorylation state or the presence of ATP. However, the native phosphorylated SA requires three-fold higher force to unfold by AFM than dephosphorylated SA, suggesting a less pliant as well as larger structure when phosphorylated.

Key words: Neurofilament; Sidearm; Phosphorylation; Intermediate filament

1. Introduction

Neurofilaments (NF) are neuron-specific intermediate filaments formed by the copolymerization of three subunits: neurofilament light chain (NF-L, 61 kDa), medium chain (NF-M, 90 kDa) and heavy chain (NF-H, 110 kDa). Unlike other cytoskeletal polymers which form smooth filaments with little self-interaction in the absence of accessory proteins, NF bear lateral extensions orthogonal to the polymer axis, sidearms (SA), which are part of a filamentous scaffolding interconnecting individual NF within neurites [1,2]. The long C-terminal domains of the NF-M and NF-H subunits form the lateral SA projections of NF [3].

The physiological functions of SA are not yet established. SA may contribute to the spacing between cytoskeletal polymers, by electrostatic [4,5] and/or steric repulsion [6,7]. The latter hypothesis requires SA to be a largely unstructured, random coil polypeptide. Alternatively, parallel associations between cytoskeletal elements within a bundle may involve attractive interactions between projections and either the core or the projections of adjacent polymers. While only NF have SA composed of the same polypeptide that forms the polymer core, other cytoskeletal filaments, notably microtubules (MT), have similar projections of large flexible binding proteins, specifically MAP2 (microtubule associated protein 2) and tau. Such cross-bridges are evident by electron microscopy between NF and NF, NF and MT, and MT and MT [1,2].

The possibility that repulsion and attraction occur simultaneously or alternatively in situ is raised by a series of apparently contradictory observations on NF bundling. It appears that NF can either spread as independent polymers from neurites of cultured neurons after dissolution of the plasma membrane [8], or NF can be isolated as tightly interconnected bundles from mature neurites of cultured neuroblastoma [9] as well as from neurons of adult mammals [9,10]. Studies of transfected cells with complete or truncated forms of NF-M or NF-H subunits further established that inter-NF cross-bridges similar to those observed in normal NF bundles in situ [1,2] depend upon the presence of critical SA domains [11,12].

One likely regulatory mechanism of SA interactions is their phosphorylation level. Multiple phosphorylation sites are located within a central domain of both NF-M and NF-H projections. A prominent substrate for phosphorylation is the lysine–serine–proline motif, the KSP domain [13] where S-phosphorylation would change the net charge of this triplet from +1 to −1.

Adenine nucleotides may also alter SA interactions based on the influence of adenosine triphosphate (ATP) on interactions between NF and MT. A mixture of NF and MT has been shown by Williams and coworkers to have an increased viscosity as ATP is added [14]. However, the same group [15] as well as Minami and Sakai [16] later found that highly viscous gels of NF and MT could also be formed in the absence of ATP. Furthermore, the possibility of an ATP-dependent regulatory mechanism of NF interactions is supported by gelation experiments involving pure NF [17], which may reveal a NF-associated ATPase activity [18].

*Corresponding author. Fax: (1)-215-5736815.
E-mail address: helim@mail.med.upenn.edu (H. Aranda-Espinoza).
[1] Equal contributors to this work.
Abbreviations: aa, amino acid; AFM, atomic force microscopy; ATP, adenosine triphosphate; DLS, dynamic light scattering; MAP, microtubule associated proteins; NF, neurofilaments; NF-L, neurofilament light chain; NF-M, neurofilament medium chain; NF-H, neurofilament heavy chain; MT, microtubules; RB, reassembly buffer; SA, sidearms; p-SA, phosphorylated sidearms; p-SAT, phosphorylated sidearms plus ATP; dp-SA, dephosphorylated sidearms; I27, human cardiac titin I band module 27; SDS–PAGE, sodium dodecyl sulfate polyacrylamide gel electrophoresis

0014-5793/02/$22.00 © 2002 Published by Elsevier Science B.V. on behalf of the Federation of European Biochemical Societies.
PII: S0014-5793(02)03515-9

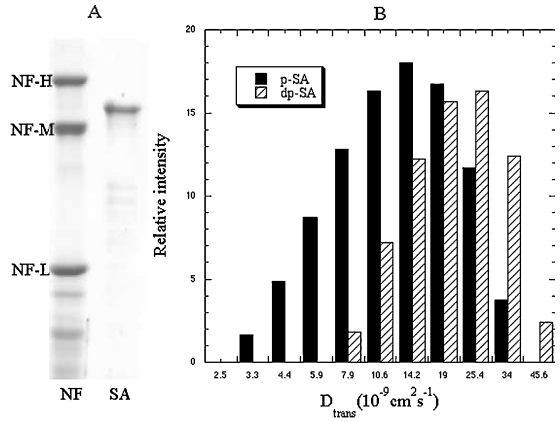

Fig. 1. A: SDS–PAGE of NF showing the proteins NF-H, NF-M, NF-L, and the SA coming from NF-H. B: Relative intensity histogram for phosphorylated (black columns) and dephosphorylated (hatched columns) SA as a function of translational diffusion coefficient.

In this paper, we offer some structural insights into SA function by studying the folded structure and the extensible stability of purified NF-H SA. Dynamic light scattering (DLS) of SA solutions and forced extensions of isolated SA by atomic force microscopy (AFM) are probed as a function of phosphorylation and solution ATP levels.

2. Materials and methods

2.1. SA preparation and dephosphorylation

Bovine NF were isolated according to [19]. Briefly, purified NF were extensively dialyzed against reassembly buffer (RB) (0.1 M morpholinoethane sulfonic acid, 1 mM $MgCl_2$, 1 mM EGTA, pH 6.8) plus 0.8 M sucrose before storage at −70°C after rapid freezing in liquid nitrogen. To obtain SA, 7.125 mg of NF was incubated with 11.2 U agarose-bound α-chymotrypsin (Sigma) for 1 h at 30°C under constant mixing, and 2.6 mM phenylmethylsulfonyl fluoride (PMSF) was added to stop the reaction. Solubilized SA were recovered in the supernatant following centrifugation at $10^5 \times g$ for 1 h at 4°C. Fractions were analyzed by sodium dodecyl sulfate polyacrylamide gel electrophoresis (SDS–PAGE) (7.5% acrylamide), showing that the SA fraction contains about 95% pure NF-H SA and a negligible amount of NF-M SA, see Fig. 1A. To dephosphorylate SA, 50 μg of NF-H SA was incubated in RB plus 1 mM PMSF for 4 days at 4°C under constant agitation together with 125 U agarose-bound alkaline phosphatase (Sigma), previously washed with nano-pure water and RB. Agarose-bound enzyme was removed by centrifugation for 5 min at $5000 \times g$. Finally, both untreated native (phosphorylated) and dephosphorylated NF-H SA were dialyzed against RB, 0.8 M sucrose, 1 mM PMSF, giving a final concentration of 0.1 mg/ml.

2.2. Dynamic light scattering

The translational diffusion coefficient of SA was measured by DLS using a DynaPro 99 instrument (Protein Solutions, Charlottesville, VA, USA), see Fig. 1B. Typically, 50 μl of SA in RB buffer plus 0.4 mM sucrose was analyzed. Phosphorylated and dephosphorylated SA with and without 1 mM ATP were studied. The translational diffusion coefficient was then used to calculate the size of SA assuming that they have a cylindrical shape [20].

2.3. AFM experiments

A 50 μl drop of 0.05 mg/ml SA was deposited on freshly cleaved mica. Protein was allowed to adsorb for 15 min and excess was rinsed away with suitable buffer. The sample was then placed without drying in the liquid cell of an AFM (Nanoscope IIIa Multimode AFM, Digital Instruments, Santa Barbara, CA, USA) with sharpened silicon nitride cantilevers (Park Scientific, Sunnyvale, CA, USA) of nominal spring constant $k_C = 10$ pN/nm. k_C was measured for each cantilever using the forced resonance method [21], with additional calibrations performed as described previously [22]. Vertical displacements were calibrated to 2 nm with a VLSI Standard having an 18 nm step height (Model STS2-180P, VLSI Standard, San Jose, CA, USA). Experiments (at ~23°C) were typically done at imposed displacement rates of 1 and 5 nm/ms. In each experiment thousands of surface-tip contacts (4000 or 6000) were collected and analyzed. Initial results were compared with results at the end of an experiment and appeared similar, indicating that there was no protein degradation or accumulation on the cantilever.

3. Results and discussion

Initial perspective on structural properties of SA is given by the amino acid (aa) sequence. Based on the homologous aa sequence from human NF-H [13], the number of residues in SA studied here is either 606 or 600, depending on the phenylalanine site where the polypeptide is cut by protease. Without loss of generality we take $N = 600$ as the total number of aa in SA. Therefore, the fully stretched length of SA is $L = Nl = 216$ nm, where $l = 0.36$ nm is the length per extended aa [23]. When dephosphorylated, the polypeptide is practically neutral (net charge −1) but the charges are unequally distributed, with a highly anionic region emanating from the filament core and a cationic region at the distal end. When SA is hyperphosphorylated (there are 76 potential phosphorylation sites) it can become highly charged (up to −153); Jaffe et al. [24] characterized 38 phosphorylation sites in NF-H. Assuming the latter phosphorylation, the SA displays a striking gradient in negative charge density that decreases from the filament core to the end of the SA, Fig. 2. Notice that charge is different principally in the central region of the SA, where most of the KSP repeats are located. With the idea that like charges repel each other, one might predict that the phosphorylated protein is larger than the dephosphorylated one.

Consistent with the expectations based on charge, the hydrodynamic sizes of isolated phosphorylated SA (p-SA) and dephosphorylated SA (dp-SA) estimated in solution from DLS (see Section 2 and Fig. 1B) are, respectively, $L_{p-SA} \approx 100$ nm and $L_{dp-SA} \approx 50$ nm. Likewise, rotary shadowing microscopy [25] of intact NF showed p-SA and dp-SA as cylindrical polypeptides with lengths $L_{p-SA} = 92 \pm 18.9$ nm

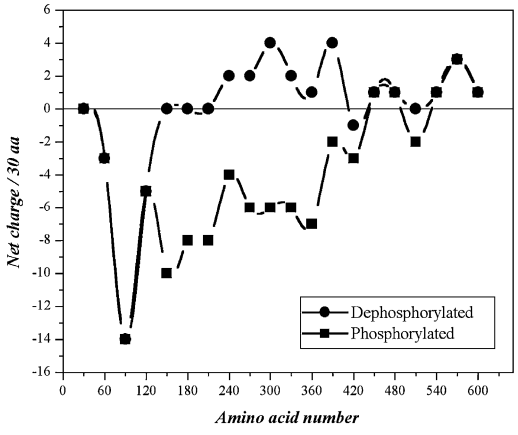

Fig. 2. Charge distribution along the SA from N- to C-terminus. Each point represents the net charge along 30 amino acids. Phosphorylated (squares) and dephosphorylated (circles) SA show a common negative region up to 120 aa. Farther away from the NF dephosphorylated is mostly positive, whereas phosphorylated is negative in the middle part and positive in the last 120 aa. Solid lines are guides to the eye.

and $L_{dp-SA} = 61 \pm 15.2$ nm, respectively. Either result corresponds to an elongation of the SA by 50–100% upon phosphorylation. DLS of both p-SA and dp-SA with 1 mM ATP revealed no significant size differences, indicating that ATP does not alter the overall shape of either p-SA or dp-SA. Following these initial insights into structure, we pursued measurements of extensibility under similar conditions.

SA were extended off of mica surfaces by AFM. It is well illustrated in the literature that pulling on a simple polymer gives extensions that grow monotonically with force [26]. In contrast, pulling on a protein with secondary and tertiary structure yields a sawtooth pattern of force versus extension, which represents forced unfolding events [22,27]. Sawtooth patterns were observed for SA under all conditions: p-SA, dp-SA, and p-SA plus 1 mM ATP (p-SAT) (Fig. 3). As the cantilever approaches the surface it might or might not interact with a molecule; if not, the number of sawtooth peaks observed (N_{pk}) = 0. If the cantilever interacts with a SA molecule, however, there is an initial desorption force that is represented by the first peak. Subsequent peaks indicate extension and unfolding of independently folded units or domains in the SA, except for the last peak, which corresponds to final desorption of the molecule from either the surface or the cantilever. Therefore, extension curves that exhibit a maximum of N_{pk} peaks correspond to $N_{pk}-2$ domains. The results shown in Fig. 3 therefore suggest that SA are composed of several structured and mechanically detectable domains.

Statistical analyses of thousands of extension curves for the three cases studied here show a maximum number of peaks $N_{pk} = 6$, thus revealing at least four domains (Fig. 4A). All cases examined showed the same number of domains. Note

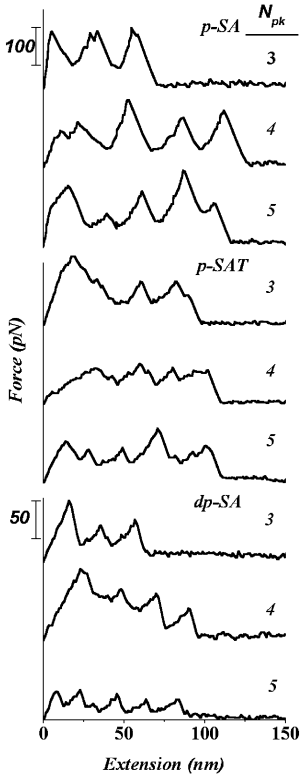

Fig. 3. Typical force-extension curves for phosphorylated sidearms (p-SA), phosphorylated plus ATP (p-SAT), and dephosphorylated (dp-SA). The imposed rate of extension was 1 nm/ms.

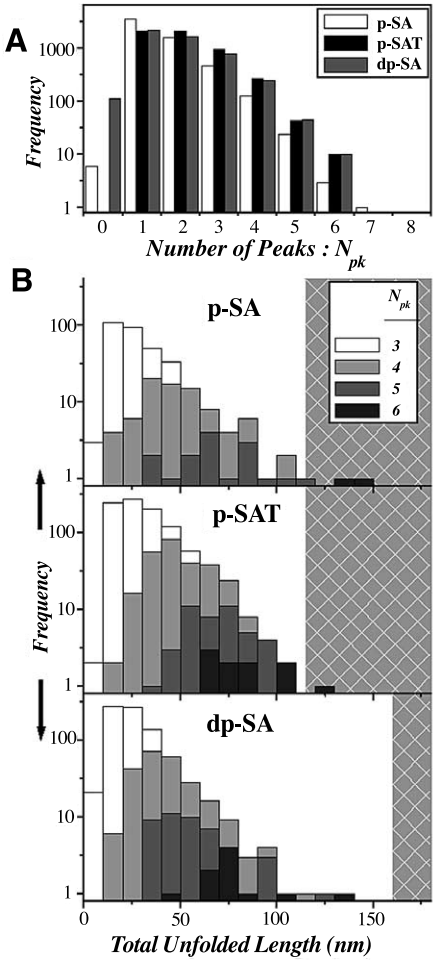

Fig. 4. Extension curve statistics for 4000 (p-SA) or 6000 (p-SAT and dp-SA) contacts of AFM tip to substrate. A: Number of peaks per extension for p-SA, p-SAT, and dp-SA. For all the conditions studied there are a maximum of six unfolding peaks and the statistics obtained are quite similar. B: Distributions of total unfolding length. These were obtained from the length of the sawtooth-shaped extension curves beyond the first (non-specific) peaks. The limit, L_u, corresponding to the full unfolding length of the SA is defined by the difference of the fully stretched contour length of the SA minus the folded length obtained by DLS.

that $N_{pk} = 7$ or 8 are zero, except for $N_{pk} = 7$ for p-SA which showed only one event. Thus, ATP and phosphorylation have no effect on the number of domains. On the other hand, dephosphorylation of p-SA was shown to decrease the native size of the SA. Total unfolding length histograms for SA (Fig. 4B) are clearly bounded by single SA contour length limits corrected as the total unfolding length $L_u = L - L_{p-SA} = 116$ nm (322 aa) for p-SA and p-SAT and $L_u = L - L_{dp-SA} = 166$ nm (461 aa) for dp-SA (gray hatched region). The absence of unfolding events larger than L_u indicates that there are no protein aggregates. Importantly, the total unfolding length obtained for SA in each type of experiment is nearly the same, indicating that there is no difference in the number of aa unfolded in each case.

Distributions of unfolding lengths between peaks (Fig. 5A) as well as the unfolding force peaks (Fig. 5B) appear largely independent of the number of peaks in an extension curve. This result is consistent with a random desorption process; it might be fitted with multiple Gaussians (e.g. four of equal

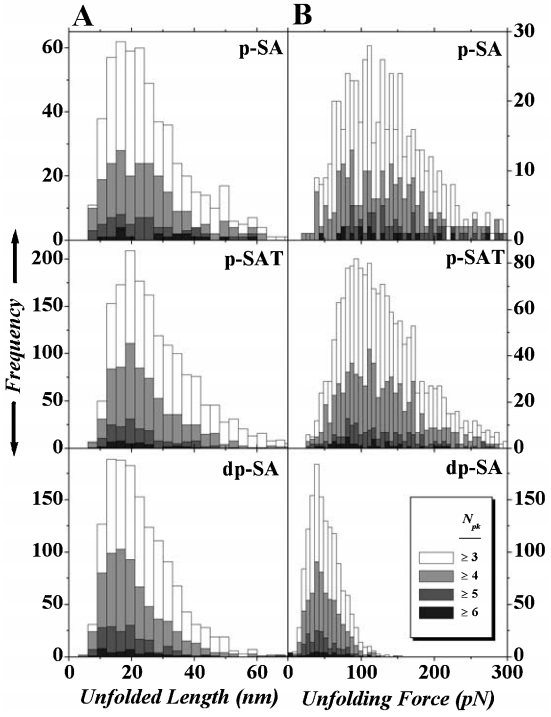

Fig. 5. Peak-to-peak unfolding lengths and forces for ensembles of extension curves. A: Length distributions for p-SA, p-SAT, and dp-SA. B: Force distributions. Average forces for p-SA and p-SAT are equal. For dp-SA the average force obtained is clearly smaller than the force for p-SA.

amplitude), but we prefer to highlight just the mean unfolding lengths. For all three cases, the mean unfolding length is approximately $D_u = 22 \pm 9$ nm, corresponding to unfolding 61 ± 25 aa. This suggests that 244 ± 100 aa are involved in the unfolding of the four SA domains. This mean number of residues involved in unfolding is thus less than the number of residues involved in the total unfolding of p-SA and p-SAT ($\sim$322 aa) or dp-SA ($\sim$461 aa). We presume that the extra aa involved in unfolding SA comes from linkers between domains of up to 78 aa for p-SA and p-SAT and 217 aa for dp-SA.

Unfolding force distributions (Fig. 5B) show a mean value of 117 ± 50.3 pN for both p-SA and p-SAT. This result, together with Fig. 3B, demonstrates that ATP has no effect on the size, number of domains, or extensible compliance of SA. In contrast, the mean unfolding force per domain for dp-SA is only 46 ± 20.5 pN. As emphasized before, dephosphorylation shows no effect on the number of domains (Fig. 4A), nor the unfolding length per domain (Fig. 5A), though it clearly weakens the domain structure. From a simple electrostatic perspective, this result might seem contradictory since it would be expected that pulling on a highly charged polymer is easier than pulling on a neutral one. However, we are pulling on a polyampholyte. Serine phosphorylation changes the KSP repeat from +1 to −1, and this can lead to new electrostatic bridges with other positively charged aa in the polypeptide. In particular, looping phosphate interactions between the KSP repeat with neighboring repeat lysine might be facilitated by the turn-inducing proline [28,29]. Fig. 6 shows a simplified cartoon of the phosphate bridge proposed. The KSPXK repeat in dp-SA forms part of the almost neutral polyampholyte and pulling on this segment should be relatively easy. However, when dp-SA is phosphorylated an electrostatic or phosphate bridge is formed between the two positive lysines in the KSPXK repeat and the two negative charges of a phosphoserine located elsewhere in the multiply phosphorylated polypeptide chain. Pulling on this phosphate bridge is more difficult, as represented by the arrows in Fig. 6. Such a mechanism accounts for the increased force required to unfold p-SA and is consistent with a previous hypothetical scheme for folded regions in the KSP and KEP domains based on secondary structure predictions [25].

Circular dichroism (CD) measurements have shown that SA (from ox) have only 20% alpha helix structure [30] (beta sheet content was not reported), in agreement with secondary structure predictors for human SA, which predicts 19.3% alpha helix, 3.6% beta sheet, and 70.8% random coil. The results here suggest a higher percentage of 24–57% (244 ± 100 aa out of 600 aa) of unfoldable aa. Comparisons to spectrin prove instructive. Despite its widely known three-helix repeat structure, CD shows spectrin to be only $\sim$70–75% alpha helix [31]. Crystal structures [32] as well as nuclear magnetic resonance [33] reveal dynamic flexible loops, which interconnect spectrin's helices. AFM has already shown that these $\sim$106 aa repeats are unfoldable, with evidence of both partial unfolding and single repeat unfolding [34,35]. Unfolding spectrin's helix-and-loop structures yields $D_u \sim$ 15–45 nm at forces generally < 50 pN. The diversity of spectrin unfolding processes is also consistent with broad distributions for SA in comparison to a protein such as titin, which shows far narrower distributions in both unfolding force (human cardiac titin I band module 27 (I27) has 204 ± 26 pN) and D_u [27,36]. Heterogeneity in SA phosphorylation might be a contributing factor since the unfolding force distributions for p-SA are much broader than for dp-SA. Whether the domains detected here for SA are folded in any way like truncated spectrin repeats or are structured more as electrostatic blobs is unclear. The latter would be consistent, however, with the difference that arises with the change in charge. It would also be consistent with a prevailing hypothesis that SA are largely unstructured chains [6,7].

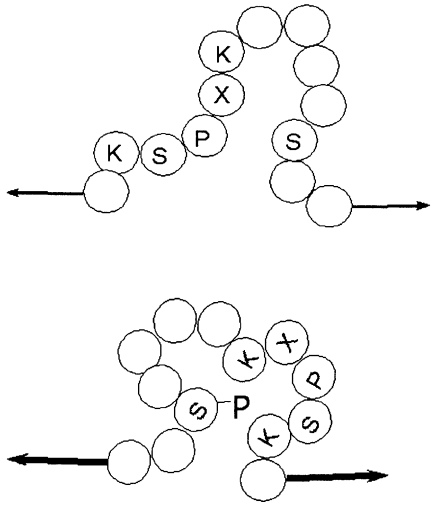

Fig. 6. Cartoon of the KSPXK repeat representing the phosphorylated and dephosphorylated configurations. The phosphate bridge increases the force required to extend the peptide segment as represented by the arrows.

In conclusion, we describe here the phosphorylation-dependent changes in the polypeptide organization of a major component of NF projections (NF-H). We also show that ATP does not influence the mechanical properties or structure of NF-H SA. Our findings indicate that SA from NF-H are both longer and less pliant when phosphorylated. The larger extended shape of p-SA may influence the effective volume occupied by the NF in the crowded intracellular space and thereby affect axon caliber. The effect of SA phosphorylation at the next level up, i.e. the rheological properties of NF and NF-MT networks, could prove revealing of such mechanisms.

Acknowledgements: H.A.E. thanks H. Bermudez and P. Photos for many insightful discussions. This work was supported by grants from the NIH/NHLBI T32HL-07954 (H.A.E.) GM56707 (P.A.J.) and Penn's NSF-MRSEC PMR00-79909 (P.A.J. and D.E.D.). P.C. and D.E.D. were supported by NIH-R01 (D.E.D.), NIH-BRP (P.C.).

References

[1] Hirokawa, N. (1982) J. Cell Biol. 94, 129–142.
[2] Hirokawa, N., Glicksman, M.A. and Willard, M.B. (1984) J. Cell Biol. 98, 1523–1536.
[3] Hisanaga, S. and Hirokawa, N. (1988) J. Mol. Biol. 202, 297–305.
[4] Marx, A., Pless, J., Mandelkow, E.M. and Mandelkow, E. (2000) Cell. Mol. Biol. 46, 949–969.
[5] de Waegh, S.M., Lee, V.M.Y. and Brady, S.T. (1992) Cell 68, 451–463.
[6] Brown, H.G. and Hoh, J.H. (1997) Biochemistry 49, 15035–15040.
[7] Kumar, S., Yin, X., Trapp, B.D., Hoh, J.H. and Paulitis, M.E. (2002) Biophys. J. 82, 2360–2372.
[8] Brown, A. and Lasek, R.J. (1993) Cell Motil. Cytoskeleton 26, 313–324.
[9] Yabe, J.T., Chylinski, T., Wang, F.S., Pimenta, A., Kattar, S.D., Linsley, M.D., Chan, W.K. and Shea, T.B. (2001) J. Neurosci. 21, 2195–2205.
[10] Shaw, G. and Hou, Z.C. (1990) J. Neurosci. Res. 25, 561–568.
[11] Nakagawa, T., Chen, J.G., Zhang, Z.Z., Kanai, Y. and Hirokawa, N. (1995) J. Cell Biol. 129, 411–429.
[12] Chen, J., Nakata, T., Zhang, Z. and Hirokawa, N. (2000) J. Cell Sci. 113, 3861–3869.
[13] Shaw, G. (1998) Neurofilaments, Springer, New York.
[14] Runge, M.S., Laue, T.M., Yphantis, D.A., Lifsics, M.R., Saito, A., Altin, M., Reinke, K. and Williams, R.C.Jr. (1981) Proc. Natl. Acad. Sci. USA 78, 1431–1435.
[15] Aamodt, E.J. and Williams Jr., R.C. (1984) Biochemistry 23, 6031–6035.
[16] Minami, Y. and Sakai, H. (1986) FEBS Lett. 195, 68–72.
[17] Leterrier, J.F., Eyer, J., Weiss, D.G. and Lindén, M. (1991) in: The Living Cell in Four Dimensions (Paillotin, G., Ed.), pp. 91–105, American Institute of Physics Conference Proceedings 226.
[18] Eyer, J., McLean, W.G. and Leterrier, J.F. (1989) J. Neurochem. 52, 1759–1765.
[19] Leterrier, J.F., Kas, J., Hartwig, J., Vegners, R. and Janmey, P.A. (1996) J. Biol. Chem. 271, 15687–15694.
[20] Doi, M. and Edwards, S.F. (1986) The Theory of Polymer Dynamics, p. 297, Oxford University Press, New York.
[21] Sader, J.E., Larson, I., Mulvaney, P. and White, L.R. (1995) Rev. Sci. Instrum. 66, 3789–3798.
[22] Carl, P., Kwok, C.H., Manderson, G., Speicher, D.W. and Discher, D.E. (2001) Proc. Natl. Acad. Sci. USA 98, 1565–1570.
[23] Creighton, T.E. (1984) Proteins, pp. 4, Freeman and Co., New York.
[24] Jaffe, H., Veeranna, Shetty, K.T. and Pant, H.C. (1998) Biochemistry 37, 3931–3940.
[25] Gou, J.P., Gotow, T., Janmey, P.A. and Leterrier, J.F. (1998) Med. Biol. Eng. Comput. 36, 371–387.
[26] Al-Maawali, S., Bemis, J.E., Akhremitchev, B.B., Leecharoen, R., Janesko, B.G. and Walker, G.C. (2001) J. Phys. Chem. B 105, 3965–3971.
[27] Rief, M., Gautel, M., Oesterhelt, F., Fernandez, J.M. and Gaub, H.E. (1997) Science 276, 1109–1112.
[28] Sharma, P., Barchi, J.J., Huang, X., Amin, N.D., Jaffe, H. and Pant, H.C. (1998) Biochemistry 37, 4759–4766.
[29] Otvos Jr., L., Hollosi, M., Perczel, A., Dietzschold, B. and Fasman, G.D. (1988) J. Protein Chem. 7, 365–376.
[30] Chin, T.K., Eagles, P.A.M. and Maggs, A. (1983) Biochem. J. 215, 239–252.
[31] LaBrake, C.C., Wang, L., Keiderling, T.A. and Fung, L.W. (1993) Biochemistry 32, 10296–10302.
[32] Grum, V.L., Li, D., MacDonald, R.I. and Modragon, A. (1999) Cell 98, 523–535.
[33] Pascual, J., Pfhul, M., Walther, D., Saraste, M. and Nilges, M. (1997) J. Mol. Biol. 273, 740–751.
[34] Rief, M., Pascual, J., Saraste, M. and Gaub, H.E. (1999) J. Mol. Biol. 286, 553–561.
[35] Lenne, P.F., Raae, A.J., Altmann, S.M., Saraste, M. and Horber, J.K.H. (2000) FEBS Lett. 476, 124–128.
[36] Carrion-Vazquez, M., Oberhauser, A.F., Fowler, S.B., Marszalek, P.E., Broedel, S.E., Clarke, J. and Fernandez, J.M. (1999) Proc. Natl. Acad. Sci. USA 96, 3694–3699.